The Journal of Experimental Biology 209, 891-906
Published by The Company of Biologists 2006
doi:10.1242/jeb.02054

Critical temperatures in the cephalopod *Sepia officinalis* investigated using *in vivo* ^{31}P NMR spectroscopy

Frank Melzner*, Christian Bock and Hans-O. Pörtner
Alfred-Wegener-Institute for Marine and Polar Research, Am Handelshafen 12, 27570 Bremerhaven, Germany
*Author for correspondence (e-mail: fmelzner@awi-bremerhaven.de)

Accepted 20 December 2005

Summary

The present study was designed to test the hypothesis of an oxygen limitation defining thermal tolerance in the European cuttlefish (*Sepia officinalis*). Mantle muscle organ metabolic status and pH_i were monitored using *in vivo* ^{31}P NMR spectroscopy, while mantle muscle performance was determined by recording mantle cavity pressure oscillations during ventilation and spontaneous exercise.

Under control conditions (15°C), changes in muscle phospho-L-arginine (PLA) and inorganic phosphate (P_i) levels could be linearly related to frequently occurring, high-pressure mantle contractions with pressure amplitudes (MMPA) of >0.2 kPa. Accordingly, mainly MMPA of >2 kPa affected muscle PLA reserves, indicating that contractions with MMPA of <2 kPa only involve the thin layers of aerobic circular mantle musculature. On average, no more than 20% of muscle PLA was depleted during spontaneous exercise under control conditions.

Subjecting animals to acute thermal change at an average rate of 1 deg. h^{-1} led to significant P_i accumulation (equivalent to PLA breakdown) and decrements in the free energy of ATP hydrolysis ($dG/d\zeta$) at both ends of the temperature window, starting at mean critical temperatures (T_c) of 7.0 and 26.8°C, respectively. Frequent groups of high-pressure mantle contractions could not (in the warm) or only partially (in the cold) be related to net PLA breakdown in mantle muscle, indicating an oxygen limitation of routine metabolism rather than exercise-related phosphagen use. We hypothesize that it is mainly the constantly working radial mantle muscles that become progressively devoid of oxygen. Estimates of very low $dG/d\zeta$ values (–44 kJ mol^{-1}) in this compartment, along with correlated stagnating ventilation pressures in the warm, support this hypothesis. In conclusion, we found evidence for an oxygen limitation of thermal tolerance in the cuttlefish *Sepia officinalis*, as indicated by a progressive transition of routine mantle metabolism to an anaerobic mode of energy production.

Key words: anaerobic metabolism, ventilation, exercise, Cephalopoda, Mollusca, mantle muscle, mantle cavity pressure.

Introduction

An oxygen limitation of thermal tolerance was proposed to be a unifying principle in ectothermic water-breathing animals (Pörtner, 2001; Pörtner, 2002a) and has been supported by the studies on several invertebrates [*Arenicola marina* (Sommer et al., 1997), *Maja squinado* (Frederich and Pörtner, 2000), *Sipunculus nudus* (Zielinski and Pörtner, 1996), *Littorina littorea* (Sokolova and Pörtner, 2003), *Laternula elliptica* (Peck et al., 2002) and the fish species *Rutilus rutilus* (Cocking, 1959), *Pachycara brachycephalum* (Mark et al., 2002) and *Gadus morhua* (Sartoris et al., 2003; Lannig et al., 2004)]. According to this hypothesis, ectothermic animals subjected to acute temperature change first experience a loss in aerobic scope and, second, oxygen deficiency beyond low and high critical temperature thresholds (T_c), ultimately leading to a transition to an anaerobic mode of energy production and time-limited survival. It was further proposed that oxygen limitation mechanisms first set in at high levels of organismal complexity, namely the integrated function of the major convection systems of the oxygen delivery apparatus.

Accordingly, previous studies have identified both ventilatory and circulatory (where present) systems in invertebrates to be limiting for oxygen transport during acute temperature change (Zielinski and Pörtner, 1996; Frederich and Pörtner, 2000), while circulatory insufficiency was suggested to be the first limiting process in fish species acutely subjected to high and low temperature extremes (Heath and Hughes, 1973; Mark et al., 2002; Lannig et al., 2004).

The present study, working with the cuttlefish *Sepia officinalis*, will focus on an animal model that, although being an invertebrate, is characterised by several vertebrate-like features. Namely, sophisticated behaviours, a closed, high-

pressure blood convection system with low blood volume and a highly efficient counter-current gill gas exchange system similar to that of fish (Wells and Wells, 1982; Wells and Wells, 1991). These features make the cuttlefish an ideal candidate to test the proposed universal character of thermal tolerance limitation mechanisms (Pörtner, 2002a).

An obvious first step is the evaluation of whether or not cuttlefish will display oxygen-limited thermal tolerance upon acute exposure to low and high temperature extremes, as evidenced by transition to an anaerobic mode of energy production at rest. Advent of mitochondrial anaerobiosis in highly aerobic liver tissue determined high T_c in fish (*Pachycara brachycephalum* and *Zoarces viviparus*), while the onset of anaerobic metabolism in white muscle only occurred shortly before death (van Dijk et al., 1999). Choice of tissues therefore seems to be crucial when investigating T_cs. Continuously working, aerobic organs with a permanently high oxygen demand are the first to suffer from oxygen deficiency and functional failure. Accordingly, we decided to monitor cephalopod mantle muscle energy status.

Cephalopod mantle tissue is permanently active and is involved in ventilatory work but also in jet-propelled locomotion: as a result, the mantle muscle evolved as a complex organ that contains thin outer layers of aerobic circular muscles, which aid during slow swimming contractions, and thick layers of anaerobic muscle fibres in the central part of the mantle muscle organ, which produce the high-pressure amplitude contractions during fast swimming (Bone et al., 1994a; Bone et al., 1994b; Bartol, 2001). The inner and outer layers of circular fibres possess high densities of mitochondria (Bone et al., 1981; Mommsen et al., 1981), leading to enhanced baseline oxygen demand. Approximately 30% of the mantle volume consists of radial muscle fibres that have a key role in ventilation (Milligan et al., 1997). By contracting, these radial muscle fibres decrease mantle muscle organ diameter to aid in refilling the mantle cavity with fresh seawater during each ventilation cycle. Funnel collar flap movements in combination with a passive relaxation of radial fibres aid during exhalation of the respiratory water. Contractions of circular muscle fibres are not involved in exhalation (Bone et al., 1994a).

Due to their permanent workload, muscle tissues active in ventilation are probably a good indicator tissue for the determination of T_cs. Other organs/tissues that are less vital during short-term stresses (i.e. digestive system, reproductive system) may even be temporarily shut down while essential fuels (nutrients, oxygen) are reallocated towards the organs that are maintained in continuous operation. Examples for such selective energy allocation towards certain organs and metabolic depression within other organs/tissues during acute environmental stressors are manifold in the animal kingdom [e.g. the mammalian diving response (Hochachka, 2000) associated with cellular metabolic depression (e.g. Buck et al., 1993)]. If, during thermal stress, anaerobic metabolism is needed to fuel ventilatory muscle contractions, obviously time-limited survival has set in and critical temperatures are being reached.

Using *in vivo* ^{31}P NMR spectroscopy, we had a technique available to continuously monitor concentrations of mantle muscle intracellular high-energy phosphate compounds and intracellular pH (pH_i) in unrestrained animals. Net utilization of the phosphagen (phospho-L-arginine, PLA) to fuel muscle contractions is a sign of the start of anaerobiosis in molluscs. We could simultaneously monitor *in vivo* performance of the very muscle fibres observed with the NMR setup by recording mantle cavity pressure oscillations. Such pressure oscillations in the mantle cavity are a consequence of rhythmic action of the mantle muscle organ's ventilatory and locomotory muscles (Bone et al., 1994a; Bone et al., 1994b).

The complexity of mantle muscle structure and the complexity of various ventilatory and locomotory functions may be confounding factors in the analysis. It was thus necessary to first learn more about the various mantle cavity pressure patterns present and their influence on muscle tissue energy status under control conditions, to later use the acquired knowledge to distinguish between (putative) effects of high-pressure mantle contractions related to spontaneous exercise and those of ventilatory pressure cycles on tissue energy status at thermal extremes.

We hypothesized that at both high and low temperatures, mantle muscle metabolism would need to switch to anaerobic metabolism during resting conditions to sustain ventilatory activity. This report therefore concentrates on muscle energy status and the effects of ventilatory activity on mantle metabolism. It will, at the same time, address the possibly interfering effects of spontaneous, exercise-related high-pressure circular muscle contractions on muscle energy status. In a companion study (F.M., C.B. and H.-O.P., manuscript submitted for publication), we analyse how the pressure patterns generated during resting ventilation relate to oxygen extraction from the ventilatory stream, metabolic rate and the costs of ventilatory movements.

Materials and methods

Animals

European cuttlefish (*Sepia officinalis* L.) used in the present study were grown from egg clusters trawled in the Bay of Seine (France) in May 2002. The animals were raised in a closed re-circulated aquaculture system (20m^3 total volume, protein skimmers, nitrification filters, UV-disinfection units) at the Alfred–Wegener–Institute on a diet of mysids (*Neomysis integer*) and brown shrimp (*Crangon crangon*) under a constant dark:light cycle (12 h:12 h) and constant temperature regime (15±0.1°C). Water quality parameters were monitored three times per week. Concentrations of ammonia and nitrite were kept below 0.2 mg l^{-1}, and nitrate concentrations below 80 mg l^{-1}. Salinity was maintained between 32 and 35‰, and water pH between 8.0 and 8.2. All animals were raised in the same 3 m^3 volume tank. Five animals (104.2±7.4 g wet mass, mean ± s.d.) were used for experimentation.

Experimental protocol

Experimental animals were starved for 24 h and then transferred to the experimental set-up. Surgery was conducted on the first day, followed by an overnight acclimatization period within the experimental chamber (control 1). *In vivo* ^{31}P NMR spectra showed that anaesthesia during surgery resulted in a transient accumulation of inorganic phosphate (P_i), which could be fully reversed within 4–6 h of recovery under control conditions. On the second day, animals were cooled from control temperature (15°C) to a lower critical temperature, then warmed to and kept at control temperature overnight (control 2), after which they were finally warmed until an upper critical temperature was reached on the third day. Temperature was changed in a stepwise procedure at an average rate of 1 deg. h^{-1}. Specifically, a 3°C temperature change was accomplished during the first hour of a 3 h period, while temperature was kept constant for *in vivo* ^{31}P NMR spectroscopy and mantle cavity pressure measurements during the two subsequent hours. Assay temperatures were 14°C/11°C/8°C on the second day, and 17°C/20°C/23°C/26°C on the third experimental day. Temperatures were changed further at a rate of 1 deg. h^{-1} if critical temperatures were not reached within the outlined temperature window. As the accumulation of P_i due to phosphagen utilization indicates limited energy production by aerobic metabolism, the appearance of significant P_i peaks in *in vivo* ^{31}P NMR spectra and their persistence over an extended time period (>60 min) defined critical temperatures.

In vivo ^{31}P NMR spectroscopy and mantle pressure oscillations

To implant a catheter for ventilatory monitoring, animals were anaesthetized with a 0.4 mol l^{-1} $MgCl_2$ solution that was mixed 1:1 with seawater (Messenger, 1985) at 15°C for 3–3.5 min, then placed (ventral side up) on a wet leather cloth to prevent skin injuries. During surgery, animals were perfused with aerated seawater (with 0.04 mol l^{-1} $MgCl_2$) through the funnel aperture. A PE cannula, required to record postbranchial pressure, was connected to a 23-gauge hypodermic needle, led through the entire mantle cavity and then fed through the posterior ventro-lateral section of the mantle muscle. Cannulae (Portex PE tubing, i.d. 0.58 mm, o.d. 0.96 mm, flared at the opening) were held in place by two 4 mm-diameter plastic washers on the inside and outside, embracing the mantle muscle in a sandwich-like fashion. PE tubes were connected to MLT-0699 disposable pressure transducers, signals were amplified with a ML-110 bridge amplifier and were further fed into a PowerLab/8SP data acquisition system (AD Instruments GmbH, Spechbach, Germany). Pressure transducers were calibrated daily.

Following surgery, animals were placed in a Perspex perfusion chamber analogous to the one used by Mark et al. (Mark et al., 2002) for eelpout (Fig. 1A). Plastic sliders within the chamber could be adjusted to the animals' dimensions and used to restrict the space available for roaming activity. The chamber was connected to a closed recirculation seawater system and placed within the magnet as described by Bock et al. (Bock et al., 2002). Water quality was maintained with a protein skimmer (Aqua Care, Herten, Germany) and a nitrification filter (Eheim Professional 2; Eheim, Deizisau, Germany). Water quality was monitored daily, and parameters were kept within the limits indicated above.

In vivo ^{31}P NMR spectroscopy experiments were conducted in a 47/40 Bruker Biospec DBX system with a 40 cm horizontal wide bore and actively shielded gradient coils (50 mT m^{-1}). A 5 cm ^{1}H/^{31}P/^{13}C surface coil was used for excitation and signal reception. The coil was placed directly under the animal chamber in such a manner as to gain maximum signal from the posterior mantle muscle section (Fig. 1B). A calculated 80–90% of sensitive coil volume was filled by mantle muscle tissue and ~10–20% by tissues from the organ sac and coelomic fluid. As *Sepia officinalis* mantle muscle tissue is characterized by high phosphagen (PLA) concentration [~34 μmol g^{-1} wet mass (Storey and Storey, 1979)], it is quite likely that the *in vivo* ^{31}P NMR spectra almost exclusively represent the adenylate pool and pH_i of the mantle musculature.

In vivo ^{31}P NMR spectra [sweep width, 5000 Hz; flip angle, 45° (pulse shape bp 32; pulse length 200 μs); repetition time (TR), 1 s; scans, 256; duration, 3 min 40 s] were acquired every 21.3 min to measure pH_i, and changes in pH_i were represented by the position of the P_i signal relative to the position of the PLA signal. pH_i was calculated using the PLA *vs* P_i shift equation obtained by Doumen and Ellington (Doumen and Ellington, 1992), using a pK_a value determined by Pörtner (Pörtner, 1990) for an ionic strength of I=0.16. pK_a values were adjusted according to temperature (Kost, 1990). ^{31}P NMR spectra were processed automatically using TopSpin V1.0 software (BrukerBioSpin MRI GmbH, Ettlingen, Germany) and a macro (written by R.-M. Wittig, AWI) to finally yield integrals of all major peaks within the spectrum (Bock et al., 2001), as these correlate with the amount of substance within the detection volume (= sensitive volume) of the ^{31}P NMR coil (Fig. 1B). Flow-weighted images to examine blood flow in major blood vessels were also generated directly before and after the collection of ^{31}P NMR spectra but will be treated separately. Concentrations of metabolites (ATP, PLA, P_i) were expressed as percentages of the total ^{31}P signal intensities. This was found necessary, as animals were free to move to some extent in the chamber both vertically and horizontally (for a maximum of 5 mm in either direction, to assure unrestrained ventilatory movements), thus altering overall *in vivo* ^{31}P NMR signal intensities:

$$[\text{Met}] = \{[\text{Met}]\,([\text{PLA}] + [\alpha\text{-ATP}] + [\beta\text{-ATP}] + [\gamma\text{-ATP}] + [P_i])^{-1}\}\,100\,, \quad (1)$$

where [Met] in % is the relative concentration of metabolite (ATP, PLA, P_i), and [PLA]+[α-ATP]+[β-ATP]+[γ-ATP]+[P_i] is the sum of the five major ^{31}P NMR peak integrals that constituted >98% of the overall ^{31}P signal (see Fig 5A). As a precondition for such an approach, it is necessary that no major phosphate export from the mantle muscle takes place. Finke et

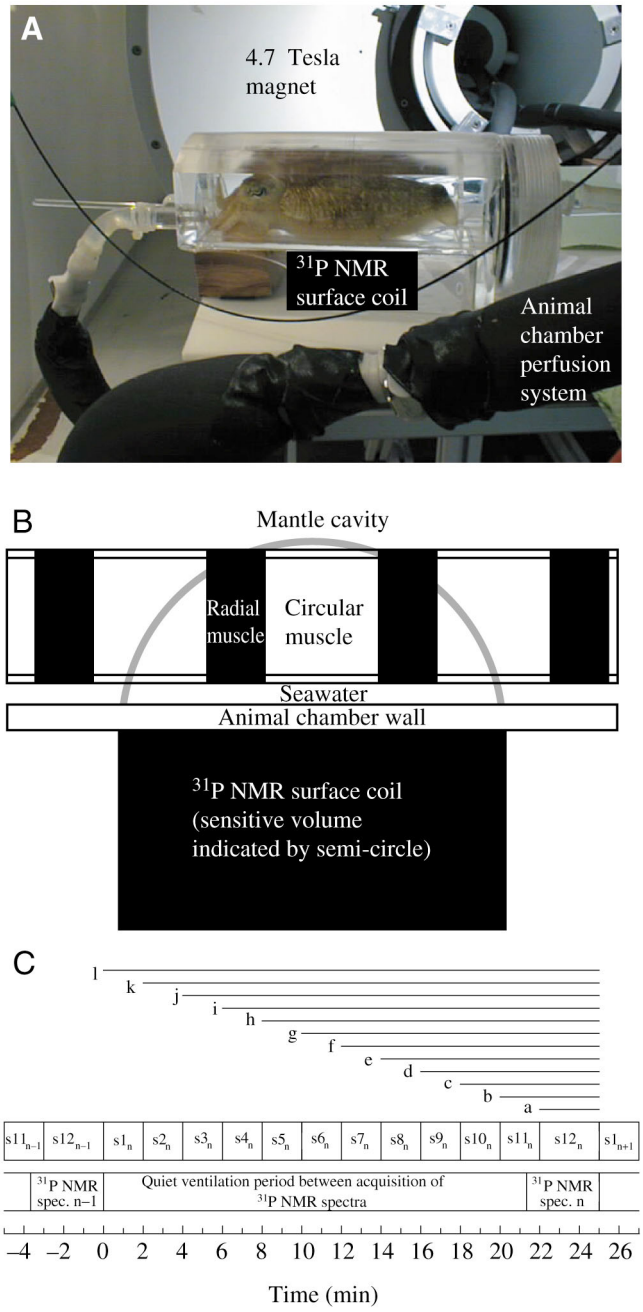

Fig. 1. (A) Animal in chamber in front of the magnet, connected to a seawater perfusion system. Sliders restrict the space available to the animal to a minimum. A grey box indicates the position of the ^{31}P surface coil below the animal's thick ventral mantle muscle. The pressure catheter (not visible) leaves the animal's mantle cavity and passes through the lid on the right towards a pressure transducer (see text). (B) Schematic illustration of the surface coil and its sensitive volume (grey semi-circle). Metabolite changes within radial and circular muscles of the mantle muscle organ can be recorded. Circular muscle consists of a central bulk of anaerobic fibres and two thin layers of outer, aerobic fibres. (C) Schematic illustration of intervals defined between the acquisition of successive *in vivo* NMR spectra. One complete 25 min interval is illustrated (n), which is divided into 12 segments ($s1_n$–$s12_n$). For each segment, swimming jet (SJ) pressure amplitudes and frequencies were determined, allowing us to calculate jet indices (JIs) for variable time intervals (by summing up segment JI within intervals a to l; e.g. interval g consists of JIs from segments $s6_n$–$s12_n$). For further explanations, see text.

al. could demonstrate that the sum of adenylates and inorganic phosphate (ATP, ADP, AMP, PLA, P_i) in squid mantle muscle (*Lolliguncula brevis*) was similar in control and exercised animals, as was the sum of all arginine-containing metabolites [PLA, octopine (Oct), L-arginine (Arg)] (Finke et al., 1996). Storey and Storey also found the sum of arginine-containing metabolites to be relatively stable in cuttlefish mantle muscle following hypoxia and exhaustive exercise (decreases of less than 10%, minor releases of Oct in the bloodstream), but they did not determine inorganic phosphate concentrations (Storey and Storey, 1979). Still, both studies suggest that anaerobic metabolites mostly remain in the mantle muscle organ in cephalopods, thus giving validity to our approach. For better visualisation, percentages of concentrations were transformed into molar quantities, assigning [PLA] control values found in cuttlefish mantle muscle (Storey and Storey, 1979) ([PLA]=33.6 μmol g^{-1} wet mass) to [PLA] controls in our study (see Table 1) and evaluating the other metabolite concentrations accordingly. Free energy change of ATP hydrolysis (dG/dζ, kJ mol^{-1}) was estimated from NMR visible metabolites as described by Pörtner et al. (Pörtner et al., 1996), with apparent equilibrium constants of arginine kinase and myokinase adjusted to changing temperatures. The identity of enthalpies of the arginine and creatine kinase reactions was confirmed by the analysis of the temperature-dependent equilibrium constant of arginine kinase under cellular conditions simulated according to Pörtner et al. (Pörtner, 1990; Pörtner et al., 1990). This analysis yielded a standard apparent enthalpy value (ΔH at pH 7.0 and 1 mmol l^{-1} free Mg^{2+}) for K_{appAK} of –11.87 kJ mol^{-1} (H.-O.P., unpublished data), which is close to the one (–11.93 kJ mol^{-1}) determined by Teague and Dobson for creatine kinase (Teague and Dobson, 1992).

Concentrations of Arg and Oct were estimated using published values (Storey and Storey, 1979) and assuming that a decrease in 1 μmol g^{-1} wet mass [PLA] results in a concomitant 0.67 μmol g^{-1} wet mass increase in [Arg] and a 0.33 μmol g^{-1} wet mass increase in [Oct] (Storey and Storey, 1979) (as witnessed during moderate and severe hypoxia and during exercise). Intracellular free [Mg^{2+}] was estimated from ^{31}P NMR spectra as described by Doumen and Ellington (Doumen and Ellington, 1992).

Mantle cavity pressure analysis

Pressure oscillations in the cephalopod mantle cavity are generated to create both a ventilatory water stream past the gills (mainly by concerted action of the collar flap muscles of the funnel apparatus and radial mantle muscles) and a jet stream to elicit swimming and escape movements (mainly by action of circular and radial mantle muscles). While the former is associated with low-pressure amplitudes, the latter can cause amplitudes of up to 25 kPa (Wells and Wells, 1991). According to Bone et al., slow swimming in cuttlefish starts

Table 1. *Control parameters (15°C) of cellular high-energy phosphates and pH_i as determined using in vivo ^{31}P NMR spectroscopy*

Parameter	Replicate 1	Replicate 2	Replicate 3	Replicate 4	Replicate 5	Mean
$[P_i]_{max}$ (μmol g^{-1} wet mass)	5.27	5.72	5.46	11.65	5.25	6.66 (2.79)
$pH_{i\ lowest}$	7.31	7.28	7.39	7.31	7.34	7.32
$pH_{i\ highest}$	7.56	7.52	7.69	7.56	7.58	7.58
$pH_{i\ range}$	0.25	0.24	0.3	0.25	0.24	0.256 (0.025)
$[H^+_i]_{range}$ (nmol l^{-1})	21.4	22.3	20.3	21.4	19.4	20.96 (1.12)
$pH_{i\ mean}$	7.43 (0.05)	7.38 (0.06)	7.50 (0.06)	7.43 (0.07)	7.44 (0.06)	7.45 (0.07)
Sig. P<0.05	3	3	1; 2; 4; 5	3	3	
$[H^+_i]$ (nmol l^{-1})	37.2 (4.38)	42.4 (5.9)	31.5 (4.0)	37.2 (6.1)	35.9 (4.4)	36.1 (5.3)
Sig. P<0.05	3	3	1; 2; 4; 5	3	3	
[PLA] (μmol g^{-1} wet mass)	33.0 (0.6)	34.5 (0.8)	33.4 (0.6)	33.8 (0.9)	33.8 (0.9)	33.6 (0.6)
Sig. P<0.05	2; 5	1; 3	2		1	
[ATP] (μmol g^{-1} wet mass)	7.3 (0.6)	8.6 (0.6)	7.9 (0.4)	8.2 (0.9)	8.1 (0.6)	8.0 (0.8)
Sig. P<0.05	2; 4; 5	1		1	1	
PLA/ATP	4.6 (0.4)	4.0 (0.4)	4.2 (0.2)	4.1 (0.5)	4.2 (0.4)	4.2 (0.4)
Sig. P<0.05	4; 5			1	1	

Statistical comparisons between animals using ANOVA and Student–Newman–Keuls *post-hoc* test. Significant differences between animals marked (e.g. sig. P<0.05=1 means that animal differs from animal 1). All results are means (s.d.). Replicates are individual animals. $[P_i]_{max}$, maximum inorganic phosphate concentration observed; $pH_{i\ lowest/highest}$, lowest/highest pH_i values observed under control conditions; PLA, phospho-L-arginine; pH_i, intracellular pH. [ATP] calculated from the β-ATP peak.

with pressure amplitudes of 0.1–1 kPa, while maximum ventilation pressure amplitudes (at rest) are 0.15 kPa (Bone et al., 1994). For an analysis of the interfering influence of spontaneous activity on temperature-dependent muscle energetics, we set a pressure threshold of 0.2 kPa as the starting point for non-ventilation-related mantle pressure generation. All such pressure oscillations will be termed 'swimming jets' (SJ) hereafter. For all five animals, frequencies of SJs of >0.2 kPa amplitude were analysed at all temperatures. In addition, mean mantle pressure amplitudes of these SJs ($MMPA_{SJ}$) were recorded (and grouped into 12 amplitude classes, i.e. 0.2–1 kPa, 1–2 kPa, […], 11–12 kPa).

3523 randomly chosen SJs from all temperatures and animals were used to develop a relationship of SJ duration *vs* measurement temperature to calculate the fraction of experimental time spent with non-ventilation pressure generation. Also, the relationship of swimming jet amplitude ($MMPA_{SJ}$) *vs* swimming jet mean pressure (MMP_{SJ} = mean pressure of SJ peaks) was determined to convert $MMPA_{SJ}$ to MMP_{SJ} at all temperatures. Routine ventilation pressures (MMP_{rout}) were analysed in similar ways. Thus, we could calculate total mean mantle pressure:

$$MMP_{tot} = [(\Delta t_1\ MMP_{SJ}) + (\Delta t_2\ MMP_{rout})]/60\ , \qquad (2)$$

where Δt_1 is the time interval (min h^{-1}) spent with swimming jets, and Δt_2 is the time interval (min h^{-1}) spent with routine ventilation.

Spontaneous exercise impacts on mantle metabolism

Mantle contractions associated with high-amplitude pressure pulses were present at all temperatures. The major challenge in the present study was thus to distinguish between the effects of spontaneous exercise and the effects of routine ventilatory mantle muscle activity (related to ventilation only) on muscle metabolic status. An extensive base of control ^{31}P NMR spectra at 15°C was available to investigate activity patterns and patterns of metabolite change in the mantle organ.

First, consecutive *in vivo* ^{31}P NMR spectra were analysed for changes in [PLA] and [ATP] parallel to changes in $[P_i]$:

$$\Delta\ [Met] = [Met]_{n+1} - [Met]_n\ , \qquad (3)$$

where Δ [Met] is the concentration change of a given metabolite, $[Met]_{n+1}$ is the concentration of the given metabolite obtained with spectrum n+1, and $[Met]_n$ is the concentration of metabolite obtained with spectrum n. Changes in pH_i were calculated in a similar fashion. A total of 282 intervals from all five animals was used for such comparisons. This was done to elaborate patterns of correlated concentration changes between the respective metabolites and pH_i and to investigate the degree to which phosphagen resources are commonly used under control conditions.

As a second step, an attempt was made to correlate metabolic changes observed within the mantle muscle with non-ventilatory muscle contractions (of pressure amplitudes >0.2 kPa). It is known from previous work that such mantle muscle contractions are fuelled in part by phosphagen breakdown, as aerobic metabolism cannot provide sufficient amounts of ATP to match demand at very high ATP fluxes (e.g. Pörtner et al., 1993; Finke et al., 1996). For this, *in vivo* ^{31}P NMR spectra were scanned for relative increases in $[P_i]$

(which is equivalent to a net phosphagen breakdown). A total of 30 intervals from all five animals was randomly selected, and all associated mantle contractions within each interval were analysed. To find a (putative) causal relationship between spontaneous exercise and metabolite changes in the mantle organ, it was necessary to identify those suitable time intervals and pressure amplitudes that actually have an effect on muscle phosphagen stores. In an exercise study on squid (*Illex illecebrosus*), it could be demonstrated that mantle phosphagen levels returned close to control levels within 10 min after fatiguing exercise, where PLA had decreased by –22.5 μmol g^{-1} wet mass from an initial concentration of >30 μmol g^{-1} wet mass (Pörtner et al., 1993). Thus, in our case, a major spontaneous exercise event, occurring 20 min prior to ^{31}P NMR spectrum acquisition, might not be reflected in the latter due to a putative rapid recovery phase of PLA stores.

Consequently, intervals (21 min 20 s between the acquisition of two ^{31}P NMR spectra plus the acquisition time of the second spectrum; thus, a total of 25 min) were divided into 11 two-minute segments and one 3 min segment (s1–s12; see Fig. 1c). Both the frequency and amplitude of SJs greater than 0.2 kPa were determined for each segment. Pressure amplitudes were grouped into classes with the following class means: 0.6 kPa (=0.2–1 kPa), 1.5 kPa (=1–2 kPa) [...] up to 11.5 kPa (=11–12 kPa) and a jet index (JI, in kPa $segment^{-1}$) obtained for each segment by adding the products of class amplitude means and jet numbers within the respective amplitude classes. For example, five jets between 2 and 3 kPa and three jets between 5 and 6 kPa within one segment yield a JI of (5×2.5)+(3×5.5)=29 kPa. 12 variables were created by adding JIs from segments within intervals ‘a’ to ‘l’ (see Fig. 1C). Furthermore, each of these variables was split up by varying the pressure threshold used for JI calculation (only jets >0.2 kPa or >1 kPa or >2 kPa, [>…], or >11 kPa used for calculations). Thus, for our example above, a JI calculated from jets >3 kPa would result in 3×5.5=16.5 kPa. This variation in duration of the interval and in the pressure amplitudes taken for JI calculation created a total of 12×12=144 different variables that could be tested in an iterative linear regression analysis to explain a maximum of the variability observed in [P_i] changes as obtained by successive *in vivo* ^{31}P NMR spectra. In a similar fashion, maximum jet density (JD) of Sjs >0.2, >1 [>...], >11 kPa within segments of intervals a to l (Fig. 1C) was calculated (again, 144 possible variables) as a second factor that might influence [P_i] changes in mantle muscle tissue. For example, JD was 15 for jets >1 kPa if we considered interval d (see Fig. 1C), and the density of jets >1 kPa (in jets 2 min^{-1}) in segments s9, s10, s11 and s12 were 9, 12, 15 and 3.

Statistics

Simple linear, exponential and sigmoidal regression analyses were performed using SigmaPlot 8.0 (SSPS Inc., Point Richmond, CA, USA). Multiple linear regression analysis was also performed using Statistica (Statsoft, Tulsa, OK, USA), as were all other statistics. Comparisons between values grouped according to temperature or animal were conducted using one-factorial analysis of variance (ANOVA) and subsequent *post-hoc* testing with Student–Newman–Keuls. *t*-tests were used to compare SJ frequencies obtained during the day with those obtained at night.

Results

Control conditions

Mantle pressure

Typical ventilation pressure amplitudes in all experimental animals were lower than 0.1 kPa, typically occurring for ⩾57 min of each control hour. The remaining time was filled with spontaneous high-pressure mantle contractions of >0.2 kPa. Occurrence of such SJs was observed in all animals, with pressure amplitudes distributed as shown in Fig. 2A. It appeared that roughly 73% of all non-routine ventilation pressure cycles of >0.2 kPa were characterized by an amplitude lower than 2 kPa. Only 0.2% of all pressure cycles of >0.2 kPa showed pressure amplitudes of 11–12 kPa.

The mean SJ pressure amplitude of all SJs >0.2 kPa was found to be 1.7 kPa. Frequencies of 108 (181) pressure cycles >0.2 kPa h^{-1} during daily (nightly) control measurements were recorded; these did not appear to be evenly distributed over time but rather were found to occur in groups of 3–50 SJs. A significant difference in high-amplitude pressure cycle frequency between night-time and daytime control measurements was also evident, with more jets observed at night (t=3.5, d.f.=4, P<0.03, N=5).

In vivo ^{31}P NMR spectroscopy

Concentrations of *in vivo* ^{31}P NMR visible metabolites and pH_i were found to be as variable as mantle pressure recordings. Fig. 3 gives an example: data are shown from 14 subsequent control ^{31}P NMR spectra taken from animal 4 between 23:22 h and 04:47 h during the second control phase of the experiment (at constant 15°C). While muscle ATP concentrations remained constant over the whole period, [PLA] decreased from 33.4 to 23.8 μmol g^{-1} wet mass (Δ[PLA]=–29%) between 50 and 100 min. This was mirrored by a concomitant increase in [P_i] from 0.8 to 11.6 μmol g^{-1} wet mass. Recovery of the phosphagen pool in combination with a decrease in [P_i] started at t=100 min and lasted for 150–200 min. pH_i values followed a similar pattern when compared with [PLA] but were delayed by ~50 min. During the first 25 min of phosphagen utilization, pH_i increased from 7.43 to 7.49. Thereafter, pH_i values decreased continuously to a minimum value of 7.32 at t=150 min. A value close to control was reached again after 325 min. The observed P_i accumulation of 11.6 μmol g^{-1} wet mass was the highest observed in any of the five animals under control conditions (Table 1).

Patterns of metabolite concentration changes and correlated pH_i changes appeared to be comparable between all animals. To elaborate these patterns, changes in metabolite concentration and pH_i were analysed from *in vivo* ^{31}P NMR

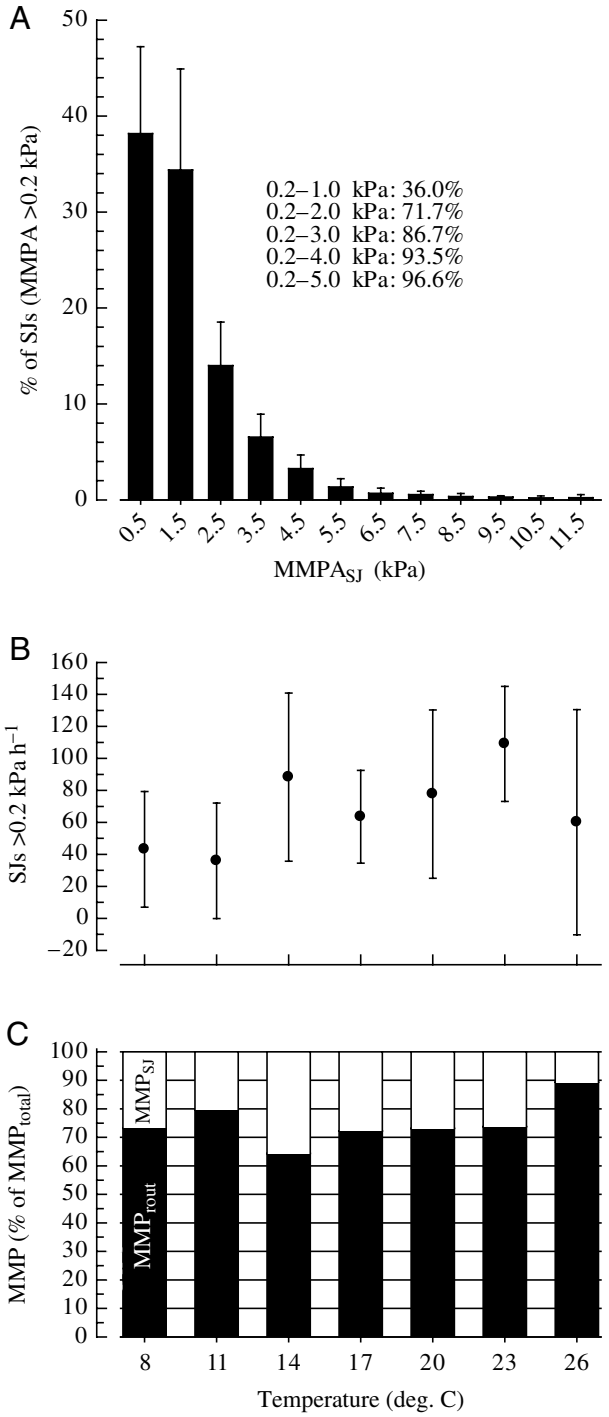

Fig. 2. Swimming jet (SJ) amplitude distribution and frequency. (A) Pressure amplitude (MMPA) distribution of spontaneously occurring high-pressure mantle cavity oscillations (SJs) of >0.2 kPa under control conditions (15°C). Amplitudes grouped into 1 kPa classes, frequencies expressed as percentage of total SJ frequency. The insert gives cumulative frequencies within selected intervals. (B) Frequency of SJs >0.2 kPa at all experimental temperatures, expressed in incidences per hour. *N*=5 animals per temperature. Error bars represent standard deviation. (C) SJ contribution to total mantle pressure generation in % of total mean mantle pressure (MMP$_{tot}$) at all experimental temperatures. See text for calculations.

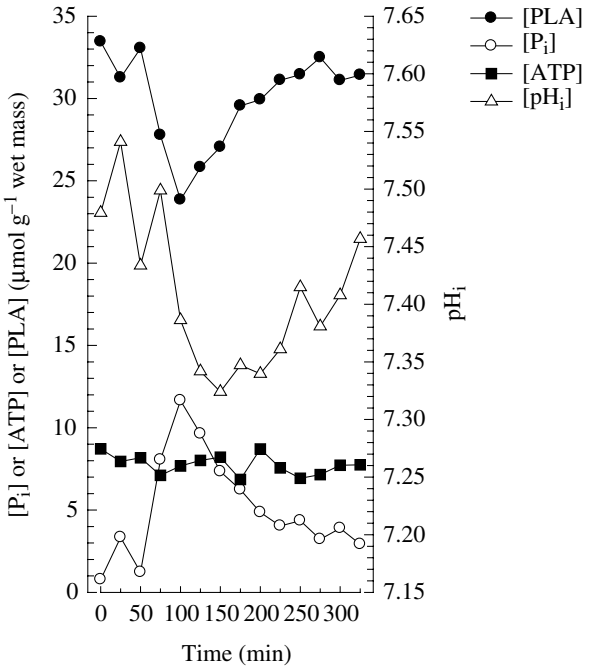

Fig. 3. Metabolite changes due to spontaneous activity under control conditions (animal 4). *In vivo* ^{31}P NMR spectra were acquired every 25 min. Each data point represents concentration information for the respective metabolite obtained from a single spectrum (acquisition time=3 min 40 s). P_i, inorganic phosphate; pH_i, intracellular pH; PLA, phospho-L-arginine.

spectra over time (Fig. 4). As would be expected from Fig. 3, Δ[PLA] changed linearly with Δ[P_i], with a negative slope close to one (Fig. 4B), while ATP concentrations remained stable at ~7–9 μmol g^{-1} wet mass (ANOVA, $F_{7,272}$=1.83, P<0.07; Fig. 4D). pH_i changed linearly with increasing Δ[P_i] between less than –3 and 3 μmol g^{-1} wet mass (Fig. 4A) but deviated significantly from this relationship once [Pi] accumulated above 3 μmol g^{-1} wet mass. pH_i fell back to 7.44 (control pH was 7.45; see Table 1) at those higher inorganic phosphate accumulations. From 282 intervals analysed for Fig. 4, only nine intervals (3%) were characterized by such a high increase in [P_i]. Correspondingly, intracellular Δ[H^+] changed linearly in the respective range of Δ[P_i] values (Fig. 4C). Increases in [P_i] of >3 μmol g^{-1} wet mass did not result in a further proton buffering but rather led to a net increase in [H^+] by 3 nmol l^{-1}.

It seemed obvious that fluctuations observed in the concentrations of high-energy phosphates and in pH_i should be related to the frequency of high-amplitude swimming jets. In a first iterative step of univariate linear regression analysis, 36 different jet index (JI) variables were identified that could explain significant fractions of variability in Δ[P_i]. These differed in the length of the time interval as well as in the pressure threshold chosen for JI calculation. Twelve of these are shown in Table 2. Intervals of 13–15 min for JI calculation (corresponding to intervals f and g in Fig. 1C) resulted in regressions with the highest r^2. Omitting mantle pressure

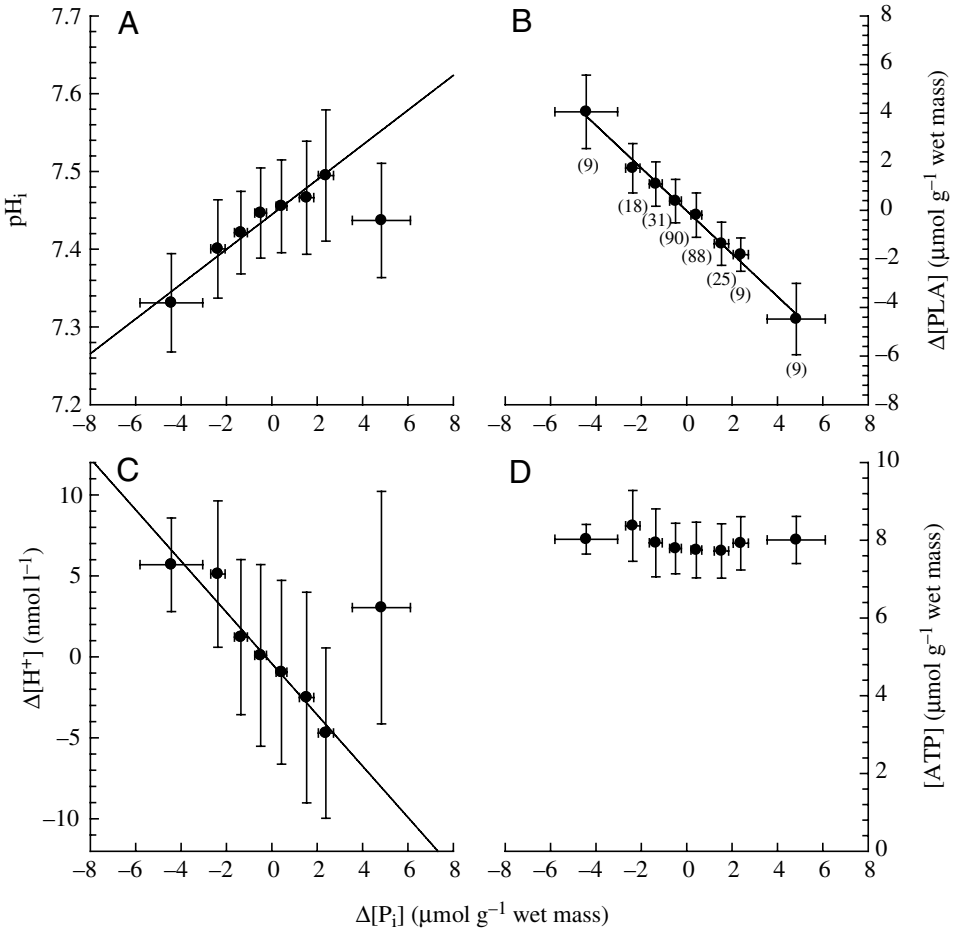

Fig. 4. Metabolite changes under control conditions. Information from N=282 intervals of 25 min duration from all five animals. Intervals were grouped according to change in inorganic phosphate between successive NMR spectra. Groups were: $\Delta[P_i]$=0–0.99 μmol g^{-1} wet mass (N=88 cases), $\Delta[P_i]$=1–1.99 μmol g^{-1} wet mass (N=25 cases), $\Delta[P_i]$=2–2.99 μmol g^{-1} wet mass (N=9 cases) and $\Delta[P_i]$=>3 μmol g^{-1} wet mass (N=9 cases) on the positive side; $\Delta[P_i]$=0 to –0.99 μmol g^{-1} wet mass (N=90 cases), $\Delta[P_i]$=–1 to –1.99 μmol g^{-1} wet mass (N=31 cases), $\Delta[P_i]$=–2 to –2.99 μmol g^{-1} wet mass (N=18 cases) and $\Delta[P_i]$=<–3 μmol g^{-1} wet mass (N=9 cases) on the negative side. Number of cases per group (displayed in B) are a direct measure of the probability of occurrence, as all intervals were picked randomly. Linear regression equations: (A) pH_i=7.444+0.022$\Delta[P_i]$; r^2=0.96, $F_{1,5}$=121, P<0.001 (for the range <–3 to 3 μmol g^{-1} wet mass); (B) $\Delta[PLA]_i$=–0.88$\Delta[P_i]$; r^2=0.99, $F_{1,6}$=222, P<0.001; (C) ΔH^+_i=–0.41–1.58$\Delta[P_i]$; r^2=0.94, $F_{1,5}$=88, P<0.001 (for the range <–3 to 3 μmol g^{-1} wet mass); (D) For ANOVA, see text. All concentrations in μmol g^{-1} wet mass (=wet mass^{-1}).

cycles below 2 kPa also resulted in better regressions, while JIs exclusively calculated from SJs greater than 3 kPa failed to explain a similar amount of variability in $\Delta[P_i]$ (Table 2). The best single variable identified was a JI constructed from mantle pressure cycles greater than 2 kPa during the last 15 min of each 25 min interval:

$$\Delta[P_i] = 0.0387\ JI\ , \quad (4)$$

where $\Delta[P_i]$ in μmol g^{-1} wet mass and JI in kPa were calculated from SJs >2kPa within interval g (see Fig. 1C). This regression could explain 84% of $\Delta[P_i]$ variability. Accordingly, 20 jets of an amplitude between 2 and 3 kPa (JI=50) would result in a $\Delta[P_i]$ of roughly 2 μmol g^{-1} wet mass, which is equivalent to a 6% decline in mantle muscle phosphagen reserves. Inclusion of a second variable, jet density (JD), into the model significantly enhanced the fraction of explainable $\Delta[P_i]$ variability to 89%:

$$\Delta[P_i] = 0.0335\ JI + 0.1555\ JD\ , \quad (5)$$

with $\Delta[P_i]$ in μmol g^{-1} wet mass and JI calculated from SJs >2 kPa within interval g, and JD calculated from jets >5 kPa within interval g (see Fig. 1C).

As high spontaneous SJs could be related to the accumulation of inorganic phosphate observed in mantle muscle, true control values for [ATP], [PLA] and pH_i were calculated only from spectra with $[P_i]$<1.5 μmol g^{-1} wet mass, as this was the maximum $[P_i]$ found during prolonged routine ventilation sequences [Table 1; only sporadic (<10) jets of pressure amplitudes of <1 kPa for at least 30 min]. Mean pH_i values were comparable between animals, except for animal 3, which showed a significantly higher mean muscle pH_i. Variability in $[H^+_i]$ was low under control conditions, with a relative standard deviation (CV) of about ±15% at a mean concentration of 36.1 nmol l^{-1}. ATP concentrations were comparable between animals 2–5, while animal 1 had a significantly lower muscle [ATP] than animals 2, 4 and 5. Although there were significant differences found in [PLA] between animals, it has to be considered that all mean concentrations were found within a range of –1.6 to +2.8% of the mean value of 33.6 μmol g^{-1} wet mass. The ratio of [PLA] over [ATP] proved to be relatively stable between animals (4.0–4.6), with ratios being comparable from animals 2–5 and only animal 1 being characterised by a significantly higher ratio (Table 1).

Acute temperature change

Mantle pressure

Bouts of spontaneous mantle muscle activity (SJs >0.2 kPa) could be observed at all temperatures (Fig. 2B), with no significant differences between temperatures ($F_{6,28}$=1.5,

Table 2. *Selected significant linear regressions of jet index vs change in inorganic phosphate concentration*

Number	X	Regression	Analysis of variance	$r^2\times100$
1	$JI_{i;\ >2\ kPa}$	$\Delta[P_i]=0.0318X$	$F_{1,28}=73.69$; $P<0.001$	72.46
2	$JI_{h;\ >2\ kPa}$	$\Delta[P_i]=0.0352X$	$F_{1,28}=106.2$; $P<0.001$	79.14
3	$JI_{g;\ >2\ kPa}$	$\Delta[P_i]=0.0387X$	$F_{1,28}=149.9$; $P<0.001$	84.26
4	$JI_{f;\ >2\ kPa}$	$\Delta[P_i]=0.0422X$	$F_{1,28}=88.88$; $P<0.001$	76.04
5	$JI_{e;\ >2\ kPa}$	$\Delta[P_i]=0.0430X$	$F_{1,28}=44.11$; $P<0.001$	62.22
6	$JI_{d;\ >2\ kPa}$	$\Delta[P_i]=0.0639X$	$F_{1,28}=35.96$; $P<0.001$	56.22
7	$JI_{l;\ >0,2\ kPa}$	$\Delta[P_i]=0.0159X$	$F_{1,28}=13.65$; $P<0.001$	30.38
8	$JI_{l;\ >1\ kPa}$	$\Delta[P_i]=0.0258X$	$F_{1,28}=27.13$; $P<0.001$	47.39
9	$JI_{l;\ >2\ kPa}$	$\Delta[P_i]=0.0515X$	$F_{1,28}=67.64$; $P<0.001$	69.67
10	$JI_{l;\ >3\ kPa}$	$\Delta[P_i]=0.0909X$	$F_{1,28}=52.90$; $P<0.001$	64.15
11	$JI_{l;\ >4\ kPa}$	$\Delta[P_i]=0.1289X$	$F_{1,28}=27.48$; $P<0.001$	47.73
12	$JI_{l;\ >5\ kPa}$	$\Delta[P_i]=0.1635X$	$F_{1,28}=16.65$; $P<0.001$	35.05
13	$X_1=JI_{15\ min;\ >2\ kPa}$		$F_{2,27}=110.7$; $P<0.001$	89.13
	$X_2=JD_{15\ min;\ >5\ kPa}$	$\Delta[P_i]=0.0335X_1+0.1555X_2$		

Regressions 1–6: variable time intervals for jet index (JI) calculation, fixed pressure threshold (only jets of >2 kPa MMPA included). Regression 7–12: variable jet amplitudes used for JI calculation, fixed time interval (25 min, interval l, Fig. 1). Regression 13 (two-factorial linear model): best model obtained, using a JI calculated for an interval of 15 min (interval g, Fig. 1) and exclusively with jets with a pressure amplitude of >2 kPa (variable X_1), the second variable being jet density (JD) of >5 kPa amplitude within interval g (variable X_2; see text for further explanations). $r^2\times100$ indicates the percentage of explained variance in $\Delta[P_i]$ (μmol g^{-1} wet mass) employing the respective regressions.

$P<0.22$). A trend towards a higher frequency of spontaneous swimming jets is evident with rising temperature between 8 and 23°C. Examination of SJs at all temperatures yielded a linear regression ($r^2=0.89$, $N=3523$ SJs) for the duration of individual SJs in relation to temperature:

$$\text{SJ duration} = -0.0225\ T + 1.3025\ , \quad (6)$$

with SJ duration in s and T representing temperature in °C. Mean mantle pressure (MMP_{SJ}) and mean mantle pressure amplitude ($MMPA_{SJ}$) were also linearly related ($r^2=0.81$, $N=3523$ SJs):

$$MMP_{SJ} = 0.2723\ MMPA_{SJ}\ , \quad (7)$$

with both MMPA and MMP in kPa. The frequency distribution of SJ amplitudes at all investigated temperatures was comparable with the one obtained during control conditions (Fig. 2A). Between 36 and 110 SJs per hour were recorded (8–26°C range), corresponding to ~1 and 3% of the total experimental time spent performing high-pressure swimming jets. With a mean SJ amplitude of 1.7 kPa (see above), the impact of relatively few high pressure cycles constituted a significant fraction of total mantle pressure (MMP_{tot}); 20–36% of MMP_{tot} were produced by high-pressure SJs (Fig. 2C) in the investigated temperature range. Owing to the high variability in SJ frequency (Fig. 2B), these differences were not significant, although a trend towards reduced pressure generation by SJs is evident between 23 and 26°C.

In vivo ^{31}P NMR spectroscopy

In vivo ^{31}P NMR spectra (Fig. 5A) revealed that despite the changes in metabolic rate and ventilatory power output observed over the entire temperature range (F.M., C.B. and H.-O.P., manuscript submitted for publication), muscle [ATP] remained constant (ANOVA; $F_{6,28}=0.13$, $P<0.99$) at around 8 μmol g^{-1} wet mass (Fig. 5B). The situation was different for the other metabolites. Although we could not detect significant differences in muscle [PLA] (ANOVA; $F_{4,20}=1.48$, $P<0.25$) and [P_i] (ANOVA; $F_{4,20}=1.68$, $P<0.20$; Fig. 5B,C) between 11 and 23°C, there was a trend towards decreasing [PLA] values between 17 and 23°C, which was mirrored by increasing [P_i] values in this respective interval. Intracellular pH decreased with rising temperature in a linear fashion ($r^2=0.87$, $F_{1,5}=33.4$, $P<0.007$):

$$pH_i = 7.528 - 0.0061\ T\ , \quad (8)$$

with T in °C (Fig. 5D). All animals started accumulating [P_i] (= net utilization of phosphagen reserves) in their mantle muscle organ at some point of time in both the cold and the warm. A huge standard deviation at 8 and 26°C indicated that the start point for this apparent failure of aerobic metabolism to sustain high cellular ATP fluxes differed between animals.

Therefore, grouping animals into pre-P_i accumulation (group A, means of *in vivo* ^{31}P NMR spectra 60 min prior to P_i accumulation) and P_i accumulation [group B, means of *in vivo* ^{31}P NMR spectra during P_i accumulation (60 min duration), with the start of accumulation defined as at least two successive spectra with a [P_i] of >1.5 μmol g^{-1} wet mass] enabled us to improve the resolution of metabolic patterns at both ends of the temperature window (Table 3). In the cold, phase B mean temperature was 7°C. From phase A to B, [PLA] had decreased to 30.9 μmol g^{-1} wet mass while [ATP] remained constant. pH_i was also comparable between phases A and B. At the warm end of the temperature spectrum, the picture was similar. At a mean temperature of 26.8°C, [PLA]

decreased to 30.5 μmol g^{-1} wet mass, while [ATP] and pHi did not change from phase A to B. Looking at the last ^{31}P NMR spectra taken at each temperature ($B_{extreme}$ in Table 3) illustrates that at high temperatures, pH_i is significantly decreased compared with phase A. A trend towards decreased pH_i values is also visible at the low-temperature $B_{extreme}$, although it is not (yet) significant. Free-energy changes of ATP hydrolysis $|dG/d\xi|$ decreased by 3.3 kJ mol^{-1} at the low temperature $B_{extreme}$ and by 5.1 kJ mol^{-1} at the high $B_{extreme}$. Mean values did not drop below 50 kJ mol^{-1}, if one assumes that phosphagen utilization is distributed evenly among all muscle fibre types [radial and circular fibres (r+c) in Table 3] present in the sensitive volume of the ^{31}P NMR coil.

Having established that changes in [PLA] and [Pi] can be caused by SJs under control conditions, it was necessary to investigate whether changes at extreme temperatures were also due to locomotory exercise or due to routine ventilation activity. Regression models were tested to establish a link between SJs and inorganic phosphate accumulation in the mantle muscle organ at extreme temperatures (phase B). Testing the same set of variables as for the control situation (see above), a significant regression model (r^2=0.49, $F_{2,29}$=14.3, P<0.001) could be established for the low extreme temperature situation

$$\Delta[P_i] = 0.022\ JI + 2.66\ JD\ , \quad (9)$$

with $\Delta[P_i]$ in μmol g^{-1} wet mass, JI calculated within interval 1 (Fig. 1C) from jets of >2kPa, and JD calculated in interval 1 from jets of >5 kPa. While this significant model could explain roughly half of the encountered variability in $\Delta[P_i]$ at low temperatures, we could not identify a single significant regression model at high temperatures.

In a second step, we looked at $[P_i]$ variability during 25 min intervals with no high-pressure jets of >0.2 kPa present. At both low and high extreme temperatures (phase B), a mean (± s.d.) accumulation of $[P_i]$ could be found (high temperature, $\Delta[P_i]$=1.15±0.3 μmol g^{-1} wet mass, N=8 intervals; low temperature, $\Delta[P_i]$=0.53±0.43 μmol g^{-1} wet mass, N=9 intervals), while during (randomly) chosen control intervals with no high-pressure cycles present, no inorganic phosphate increases could be found at all ($\Delta[P_i]$=–1.65±1.9 μmol g^{-1} wet mass, N=8 intervals). Rather, negative $\Delta[P_i]$ values dominated under control conditions, as periods without any SJs at all were found predominantly during recovery times from (spontaneous) exercise.

In summary, we have found significant increases in $[P_i]$ (= phosphagen use) in the mantle muscle organ at both high and low temperature extremes in all five animals investigated. At a control temperature of 15°C, $[P_i]$ variability could almost completely (89%) be explained by the occurrence of high-pressure SJs. At high extreme temperatures, SJs could not be related to the observed increases in $[P_i]$. Inorganic phosphate accumulation was also observed during intervals without any SJs present, and thus was likely to be caused by elevated levels of routine ventilation alone. At low extreme temperatures, apparently both processes (routine ventilation energy demands and spontaneous exercise energy demands) contributed to $[P_i]$ accumulation.

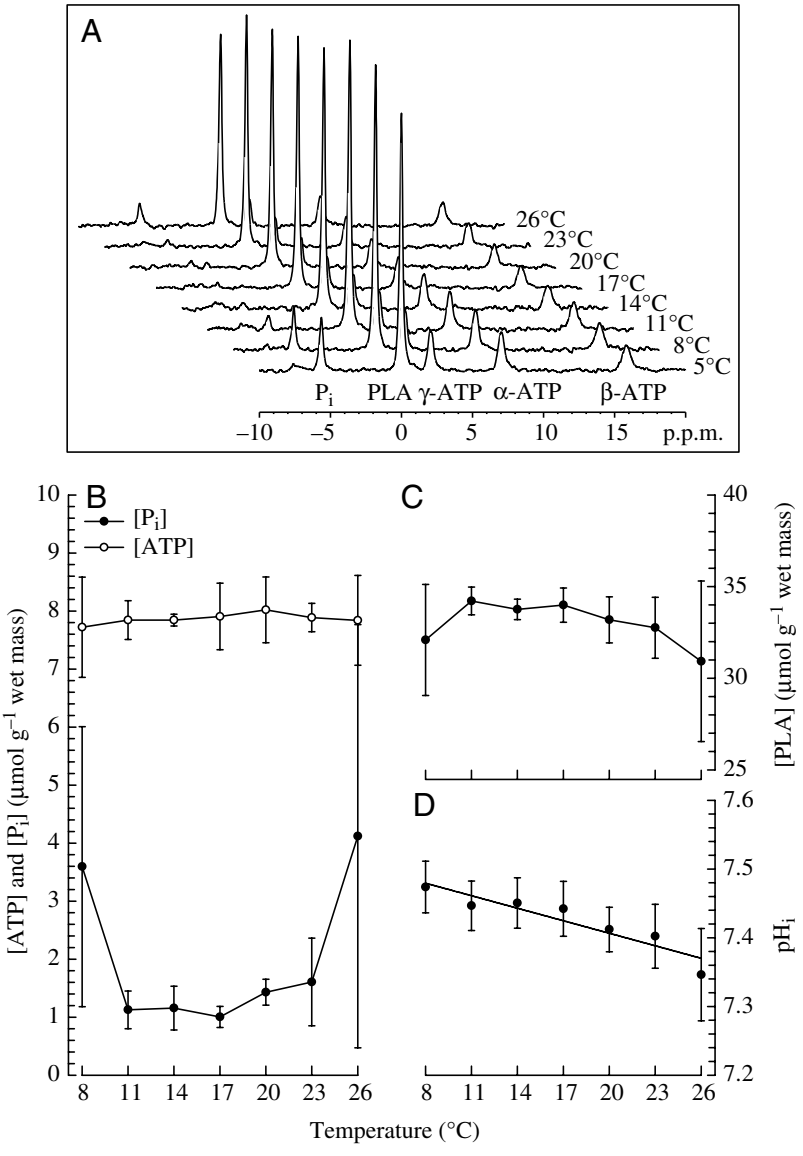

Fig. 5. Mantle organ metabolic status *vs* temperature. (A) A set of spectra obtained on animal 1 at different temperatures. Note increases in inorganic phosphate (P_i) peak area towards high and low temperatures. (B) ATP and P_i concentrations; (C) phospho-L-arginine (PLA) concentration; (D) intracellular pH (pH_i). N=5 animals per temperature. Error bars represent standard deviation. Data derived from *in vivo* ^{31}P NMR spectra. Concentrations of metabolites are proportional to the area under their respective peaks in the ^{31}P NMR spectrum.

Table 3. *Cellular energy status at extreme temperatures*

	Low extreme temperature			High extreme temperature				
	A (r+c)	B (r+c)	$B_{extreme}$ (r+c)	A (r+c)	B (r+c)	$B_{extreme}$ (r+c)	A (r)	$B_{extreme}$ (r)
pH_i	7.47 (0.04)	7.48 (0.07) n.s.	7.44 (0.06) n.s.	7.38 (0.07)	7.35 (0.04) n.s.	7.29 (0.03) *P*<0.001	7.38	7.19
[PLA] (μmol g^{-1} wet mass)	34.5 (1.2)	30.9 (2.1) *P*<0.006	30.7 (2.3) *P*<0.006	33.1 (1.2)	30.5 (2.1) *P*<0.04	28.1 (3.5) *P*<0.001	33.1	8.5
[P_i] (μmol g^{-1} wet mass)	1.3 (0.3)	4.5 (1.9) *P*<0.004	4.6 (1.8) *P*<0.004	1.2 (0.3)	4.5 (1.1) *P*<0.001	7.5 (1.2) *P*<0.001	1.2	25.6
[ATP] (μmol g^{-1} wet mass)	7.7 (1.0)	7.9 (0.5) n.s.	8.0 (1.2) n.s.	8.0 (0.4)	7.8 (1.0) n.s.	7.5 (1.2) n.s.	8.0	5.8
Temperature	9.02 (1.4)	6.97 (0.81)	6.3 (1.1)	23.1 (2.3)	26.78 (1.9)	27.2 (1.6)	23.1	27.2
[Oct] (μmol g^{-1} wet mass)	0.2	1.4	1.5	0.2	1.06	1.9	0.2	8.2
[Arg] (μmol g^{-1} wet mass)	30.4	32.8	32.9	29.1	30.8	32.4	29.1	45.5
$[Mg^{2+}]_I$ (mmol l^{-1})	1.2 (0.3)	1.1 (0.3)	1.1 (0.3)	1.8 (0.35)	1.8 (0.68)	1.8 (0.7)	1.8 (0.35)	1.8 (0.7)
d*G*/dζ (kJ mol^{-1})	–54.7	–51.3	–51.4	–55.9	–52.3	–50.8	–55.9	–44.0

See text for definition of phases and abbreviations. Differences between phase mean values were detected using ANOVA and Student–Newman–Keuls tests. Only results from *post-hoc* comparisons between group A and each other group are displayed in this table. n.s., non-significant; (r+c), metabolite levels and pH_i values assuming a homogeneous distribution over the whole mantle organ (radial and circular muscle fibres); (r), metabolite levels and pH_i values assuming a heterogeneous distribution of metabolite levels in that phosphagen depletion only took place in radial muscle fibres; extreme, values obtained with the last *in vivo* ^{31}P NMR spectrum prior to termination of cooling or heating; $[Mg^{2+}]_I$, intracellular, free magnesium, estimated using ^{31}P NMR spectra according to (Doumen and Ellington, 1992); Oct, octopine; Arg, arginine; PLA, phospho-L-arginine; pH_i, intracellular pH; P_i, inorganic phosphate; d*G*/dζ, free energy change of ATP hydrolysis. [ATP] calculated from the β-ATP peak.

Discussion

Using non-invasive *in vivo* ^{31}P NMR spectroscopy, we were able to continuously monitor key components of the *S. officinalis* mantle muscle energy system in unrestrained animals subjected to acute temperature changes. Our aim was to identify potential threshold temperatures, below or above which aerobic metabolism would insufficiently provide the energy required for muscle maintenance, routine activity (ventilatory contraction of radial fibres) and facultative exercise (high-pressure contractions performed by aerobic and anaerobic circular fibres). A number of invasive studies on cephalopod mantle organ tissue has provided the necessary information to interpret the observed changes in NMR visible metabolites ([PLA], [P_i], [ATP]) and pH_i, following the advent of anaerobic metabolism, both in mitochondria and the cytosol (Storey and Storey, 1979; Gaede, 1980; Finke et al., 1996; Pörtner et al., 1991; Pörtner et al., 1993; Pörtner et al., 1996; Zielinski, 1999; Zielinski et al., 2000).

Control conditions

During control conditions, we had the unique possibility to study the effects of facultative mantle muscle exercise on the animals' intracellular energy status. We could show that animals displayed a higher activity (as evidenced by the occurrence of SJs with an amplitude of >0.2 kPa) during 1–3% of the total time. Similar levels of activity were recently found for a tropical cuttlefish in its natural habitat [*S. apama* was found to be active (as estimated from elevated mantle pressures) for approximately 3% of the day (Aitken et al., 2005)].

Control mantle muscle organ adenylate levels obtained in our study, as witnessed by the ratio of [PLA] over [ATP], are comparable with other studies that analysed metabolite concentrations invasively. Our ratio of 4.2 (0.4 s.d.) compares well with a value of 3.9 for *S. officinalis* (Storey and Storey, 1979), 4.4 for the squid *Lolliguncula brevis* (Finke et al., 1996) or 3.5 for the squid *Loligo pealei* (Pörtner et al., 1993). We were able to clearly demonstrate that PLA stores were being utilized during high-pressure SJs and could establish a quantitative relationship between exercise levels and decreases in [PLA] or increases in [P_i], respectively. The best relationship obtained suggests that SJs with a MMPA of >2 kPa cannot be fuelled entirely by means of aerobic energy production, similar to findings in the squid *L. brevis* (Finke et al., 1996). This fits the picture that slow-swimming ('cruising') mantle pressure amplitudes in *S. officinalis* do not seem to exceed 2 kPa (fig. 1b in Wells and Wells, 1991). Bone et al. could demonstrate that during slow swimming at pressure amplitudes between 0.1 and 1.0 kPa, (aerobic) circular fibres become involved in the pressure generating process (Bone et al., 1994a). Thus, it is quite likely that slow swimming at <2 kPa can be fuelled entirely by metabolism of the thin

aerobic muscle layers of the mantle periphery. More extreme exercise with pressure amplitudes of >2 kPa progressively involves central anaerobic fibres (Bone et al., 1994b) that exploit their phosphagen reserves in order to propel the animal at higher speeds. Gradual involvement of central (mainly) anaerobic fibres (rather than an all-or-nothing transition) to support aerobic fibres at an increasing workload has been recently demonstrated for swimming squid (*L. brevis*) (Bartol, 2001).

The fact that we found a linear relationship between jet indices constructed from mantle pressure amplitudes multiplied with jetting frequencies and phosphagen use is not surprising, as pressure production should be a direct function of circular mantle muscle fibre force generation. Muscle fibre force has been found to depend on the number of crossbridges in the force generating state per cross-sectional area (e.g. Wannenburg et al., 1997); thus, mantle cavity pressure in cephalopods should be directly proportional to ATP flux rates in working mantle muscle. This corresponds to the results of Webber and O'Dor, who found correlated changes in mantle pressure integral and whole-animal rate of oxygen consumption ($\dot{M}_{O_2}$) during various levels of exercise in a squid (*I. illecebrosus*) (Webber and O'Dor, 1986).

The inclusion of a second variable into the regression model (jet density) significantly enhanced the fraction of explainable variation in inorganic phosphate concentration changes. This implies that high amplitude jets of >5 kPa pose a higher threat to cellular phosphagen reserves when they occur in quick succession, rather than distributed over a longer time interval. This could be due to oxygen depletion or aerobic fibre fatigue at high jet density, resulting in pressure generation exclusively by anaerobic fibres during high jet density, high-pressure time intervals.

It should be emphasized that PLA stores were never used extensively under control conditions (15°C) and during facultative, spontaneous exercise. Mean maximum decreases in [PLA] (= increases in [Pi]; see Table 1) under control conditions amounted to 6.66 μmol g^{-1} wet mass, which corresponds to roughly 20% of phosphagen reserves, although one animal (replicate 4, Fig. 3) depleted 35% of its phosphagen reserves on one occasion.

Fig. 3 demonstrated that during initial phosphagen transphosphorylation and P_i accumulation, pH_i can be buffered and remains unchanged. pH_i decreased only during prolonged phosphagen utilization, probably due to glycolysis and concomitant octopine formation (Storey and Storey, 1979; Pörtner, 1987; Pörtner, 2002b). Work on *in vitro* preparations of scallop (*Argopecten irradians*) contracting phasic adductor muscles supports this conclusion (Chih and Ellington, 1985). While, during initial exercise (40 muscle contractions), proton consumption by phosphagen utilization exceeded proton production by octopine formation, resulting in a net alkalosis of about 0.09 pH units ($\Delta[H+]$=–16 nmol l^{-1}), further exercise (40–200 contractions) led to progressively declining pH_i values due to glycolytic proton production outmatching proton consumption by the phosphagen. Fig. 4 provides a more quantitative picture and shows clearly that anaerobic metabolism is seldom employed to the degree that net cellular acidification occurs. Only 3% of all (randomly chosen) intervals analysed for Fig. 4 showed a $[P_i]$ accumulation of >3 μmol g^{-1} wet mass. Such a degree of phosphagen utilization goes along with the onset of muscle acidosis, suggesting that glycolytic proton production outmatches proton buffering by phosphagen use.

Apparently, cuttlefish avoid intracellular acidification by terminating exercise in most cases as soon as glycolytic proton production equals phosphagen proton buffering capacity. Upon removal of inorganic phosphate during recovery, a glycolytic proton surplus, which cannot be buffered, results in a slight decrease in pH_i (Fig. 4A,B). Potentially adverse effects of decreased pH_i values on muscle function (reviewed by Fitts, 1994) are thus shifted into recovery phases. Absolute changes in intracellular proton activities are low (in the nmole range; Fig. 4B), a feature also observed by Chih and Ellington (Chih and Ellington, 1985). A recent *in vivo* ^{31}P NMR spectroscopy study on forced scallop exercise (Bailey et al., 2003) confirmed the metabolic patterns obtained in the older *in vitro* study on stimulated adductor muscle preparations.

Acute temperature change

Fig. 5 depicts the changes in mantle organ metabolite levels with temperature. Despite the dramatic changes in ventilatory power output over the entire temperature range, [ATP] is strictly conserved (Fig. 5A), a phenomenon commonly encountered in studies on muscles of marine ectothermic animals subjected to acute temperature change (i.e. Mark et al., 2002; Sartoris et al., 2003; Zielinski, 1999) and generally referred to as the 'stability paradox' (Hochachka and Somero, 2002). [PLA] was also constant between 11 and 23°C.

We could not find any evidence for an alphastat pattern of pH_i regulation (Reeves, 1972; see Burton, 2002 for a review) in the investigated temperature range. Typically, changes of around –0.018 pH units $deg.^{-1}$ are expected to ensure constant levels of imidazol and protein ionization. For fish species, such a pattern could be demonstrated in white muscle (Borger et al., 1998; Van Dijk et al., 1997; Van Dijk et al., 1999; Bock et al., 2001). As for molluscs, an alphastat pattern of pH_i regulation was absent in the stenothermal marine bivalve *Limopsis marionensis* (Pörtner et al., 1999). Despite confounding effects of mantle muscle exercise at all temperatures, we found a decrease in pH_i with temperature by about –0.006 pH units $deg.^{-1}$ over the full temperature range examined. Omitting pH_i values at 8 and 26°C, as phosphagen utilization was observed to start at these temperatures, gives an even lower rate of change of –0.004 pH units $deg.^{-1}$. Between 11 and 17°C [the typical natural temperature range of this population of cuttlefish in the English Channel (Boucaud-Camou and Boismery, 1991)], pH_i values are nearly identical. The absolute temperature-dependent changes in pH_i are <0.05 units between 11 and 23°C, which is lower than the range of change observed during facultative exercise at control temperature. Future studies should address the time

dependence of pH_i regulation in response to temperature. Our study focused on short-term temperature effects and may not have allowed mantle pH_i to fully reach new steady-state values after each thermal challenge. As it stands, the question of temperature-dependent pH_i regulation in cephalopods must remain open.

Patterns of metabolite changes observed at extreme temperatures exactly mirrored those during exercise under control conditions. The start of phosphagen utilization was observed in all five animals at both temperature extremes during phase B. Mean temperatures during this phase were 26.8°C and 7°C.

High T_c

The analysis of mechanisms at the high end of the temperature spectrum proved to be easier than at the low end. As no relationship between the few SJs (see Fig. 2B,C) and the use of the phosphagen could be established and, also, since $[P_i]$ increases could be found during periods of ventilation at rest, obviously aerobic metabolic limitation had set in independent of effects of spontaneous SJ exercise at warm temperatures. Still, the results are difficult to interpret as mantle muscle is a complex organ that consists of different muscle fibre types with different functions (Bone et al., 1981; Bone et al., 1994a; Bone et al., 1994b; Bartol, 2001). Radial muscle fibres aid in refilling the mantle cavity during ventilation by contracting and thus enlarging mantle cavity volume. Bone et al. were the first to demonstrate (Bone et al., 1994a) that expiration in the cuttlefish under control conditions (18°C) and at rest (mantle pressure amplitudes of 0.05–0.15 kPa) is not brought about by contraction of the outer, aerobic layers of circular fibres but rather by the movements of the collar flaps (muscular funnel appendages) (see Tompsett, 1939) that expel water rhythmically from the mantle cavity. Maximum resting ventilation MMPA recorded in our experimental animals were lower than 0.15 kPa (F.M., C.B. and H.-O.P., submitted), thus we assume that during our entire experimental series, radial fibres had been the only constantly working myofilaments within the sensitive volume of our ^{31}P NMR coil (Fig. 1B). Our companion study revealed that ventilation pressures stagnate at temperatures beyond 26°C. Fig. 6A shows ventilation pressure amplitudes (at rest) at temperatures close to the upper T_c for two experimental animals (the ones with the highest and the lowest T_cs), while Fig. 6B gives correlated increases in $[P_i]$ (circles). It is quite evident from this figure that declining ventilation pressures and phosphagen use are tightly coupled (all other experimental animals showed similar patterns). We thus conclude that an energetic limitation of radial muscle fibres is responsible for the observed increases in $[P_i]$ and the correlated decreases in ventilation pressures once phosphagen usage starts. Radial fibres have a mitochondrial content as low as that of central 'anaerobic' circular fibres (Bone et al., 1981; Mommsen et al., 1981) and thus may be especially sensitive to enduring ventilation exercise at high intensities. Considering that radial fibres constitute about 30% of total mantle volume in the cuttlefish (Milligan et al., 1997), and assuming that

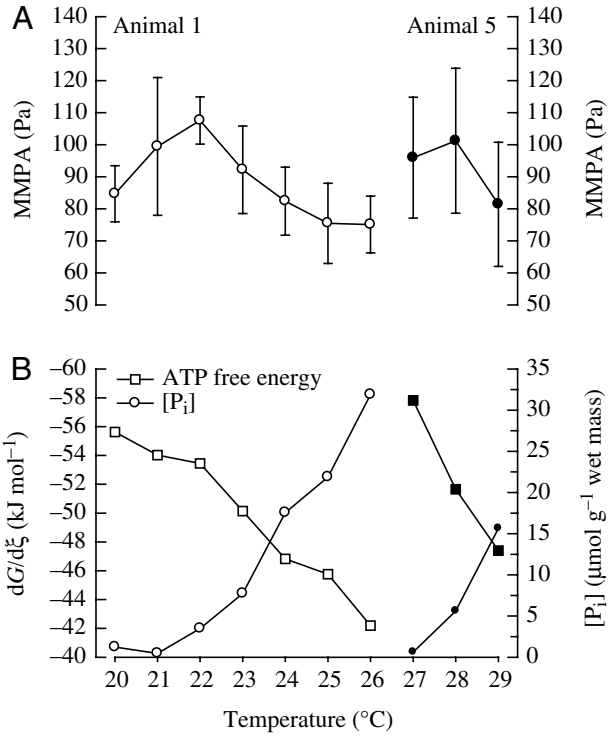

Fig. 6. Mantle metabolic status and mean mantle pressure amplitude (MMPA) *vs* temperature. (A) MMPA maxima encountered in animals 1 and 5; (B) concomitant changes in $[P_i]$ and free energy change of ATP hydrolysis ($dG/d\zeta$) in the radial muscle compartment, based on the assumption that observed changes in *in vivo* ^{31}P NMR spectra solely represent the situation in working radial muscles (see text). Animal 1 had the lowest and animal 5 had the highest thermal tolerance of all animals investigated. Still, both show a tight correlation between stagnating and, eventually, decreasing, pressure amplitudes once $|dG/d\zeta|$ decreases (the other three animals show similar patterns; data not shown).

solely radial fibres deplete their phosphagen stores as ventilation pressures increase while, on the other hand, circular fibre energy status remains constant, it is possible to estimate metabolite changes for the radial fibre compartment. Based on such considerations, radial fibre $|dG/d\zeta|$ for animals 1 and 5 would drop severely as phosphagen use proceeds (Fig. 6B). Following such a rationale, metabolite changes were recalculated for phase B (denoted r in Table 3) for all five animals. Thus, mean [PLA] reserves would decrease by 75% from 33 to 8.5 μmol g^{-1} wet mass, mirrored by an increase in $[P_i]$ in the same range and a 25% reduction in [ATP]. pH_i would be significantly decreased to 7.19 and $|dG/d\zeta|$ would drop to below 44 kJ mol^{-1} in the radial fibre compartment of the mantle organ. These calculations correspond to similar $|dG/d\zeta|$ values for mantle muscle of three species of squid following fatiguing exercise, which ranged from 42 to 47 kJ mol^{-1} (Pörtner et al., 1996), while values for two species of exercise-fatigued eelpout (*P. brachycephalum, Z. viviparous*) (Hardewig et al., 1998) white muscle ranged from 46.6 to 48 kJ mol^{-1}. Possibly, reductions in the free energy of

ATP hydrolysis as calculated for cuttlefish radial muscle could contribute to muscle fibre fatigue in that vital muscle due to functional impairments of ATPase functions. Kammermeier et al. found a drop in contractile performance of perfused rat hearts (38°C) below a $|dG/d\zeta|$ of 48 kJ mol^{-1} (Kammermeier et al., 1982). They calculated threshold values of $|dG/d\zeta|$ required for proper function of the various ATPases engaged in muscular work to range from 45 to 53 kJ mol^{-1} (Kammermeier, 1987; Kammermeier, 1993). Only recently, Jansen et al. found maintenance of $[Na^+_i]$ homeostasis prevented by $|dG/d\zeta|$ values below 50 kJ mol^{-1} due to a limitation of the sodium pump (Na^+/K^+-ATPase) in perfused rat hearts (Jansen et al., 2003). Less information on critical $|dG/d\zeta|$ values for muscle function is available for ectothermic animals: Combs and Ellington calculated an energy requirement of 41 kJ mol^{-1} for blue mussel (*Mytilus edulis*) sarcolemmal Ca^{2+}–ATPase (Combs and Ellington, 1995). A minimum $|dG/d\zeta|$ value of 46 kJ mol^{-1} for the sodium pump of crayfish abdominal muscle was calculated by the same authors (Combs and Ellington, 1997), although they found changes in $[Na^+_i]$ homeostasis well above 50 kJ mol^{-1} already. They speculated that global $|dG/d\zeta|$ might not reflect the $|dG/d\zeta|$ close to the sodium pump.

Also, both elevated intracellular proton and inorganic phosphate concentrations have frequently been connected with muscular fatigue independent of $|dG/d\zeta|$ (Allen and Westerblad, 2001; Fitts 1994). Increased $[P_i]$ is thought to reduce muscle force by reversing the force-generating P_i release step by mass action (Hibberd et al., 1985). According to Debold et al. (rat muscle fibres), the $[P_i]$ dependency of muscle fatigue is temperature related, with a more pronounced effect of $[P_i]$ at low temperatures (Debold et al., 2004). For ectothermic (marine) animals such studies have, to our knowledge, not been undertaken.

Judging from the presented results and literature data, it appears that progressive phosphagen usage is indeed causative of the observed stagnation in ventilatory pressure generation at high temperature extremes, although the exact mechanisms still need to be elucidated.

Low T_c

At low temperatures, we could demonstrate that SJs contributed significantly to increases in $[P_i]$. 50% of variability in $\Delta[P_i]$ could be attributed to facultative exercise of circular anaerobic fibres, while the other half remained unexplained. As neither SJ frequency nor the fraction of MMP_{SJ} in MMP_{tot} increased at lower temperatures (similar frequencies/pressures were observed between 8 and 11°C; Fig. 2B,C) and no P_i accumulation occurred at 11°C (Fig. 5B), a major loss in aerobic scope for spontaneous activity had evidently occurred towards low temperature extremes, resulting in the net use of phosphagen stores for spontaneous activity. The other 50% of variability that could not be explained by the linear regression is likely due to a limitation in oxygen flux towards radial muscles, thus limiting their active role in ventilation. It seems that, at low temperatures, all muscle fibre types might suffer from phosphagen breakdown. Accordingly, we calculated $|dG/d\zeta|$ values assuming that mantle phosphagen depletion took place more homogeneously. In $B_{extreme}$, $|dG/d\zeta|$ had dropped from 55 to 51 kJ mol^{-1}. This does not exclude the existence of heterogeneity or even of putative intracellular $|dG/d\zeta|$ gradients. Hubley et al. calculated distinct intracellular concentration gradients of the vertebrate phosphagen, creatine phosphate (PCr), and free energy of ATP hydrolysis in working fish white muscle, depending on the maximum distance from the nearest mitochondrion (Hubley et al., 1997). Maximum intracellular $|dG/d\zeta|$ gradients of 7 kJ mol^{-1} were calculated. Interestingly, the study suggests that in fish white muscle such $|dG/d\zeta|$ gradients will be less pronounced in animals acclimated to high temperature (25°C) and acutely exposed to low temperature (5°C). This is mainly due to differing temperature relationships of metabolic rates and intracellular diffusion coefficients for ATP and PCr (i.e. Q_{10} for D_{PCr} was only found to be 1.28, while, typically, Q_{10} values for metabolism are >2). If this holds true for cuttlefish muscle as well, we can expect drops in $|dG/d\zeta|$ to have less severe impact on intracellular ATPase function, and thus muscle function, during oxygen limitation developing at acute exposure to low temperatures.

However, although oxygen limitation of thermal tolerance in the cold likely progresses at a slower pace, phosphagen usage during periods without spontaneous activity is a certain sign of a cellular energy limitation, leading to time-limited survival of the organism.

Perspectives: thermal limitation in cephalopods vs fish

Van Dijk et al. found no changes in fish (*P. brachycephalum*, *Z. viviparus*) white muscle energy status at high critical temperatures ($|dG/d\zeta|$ did not drop below 60 kJ mol^{-1}), while in liver, an accumulation of succinate indicated a progressive switch to mitochondrial anaerobiosis (Van Dijk et al., 1999). Furthermore, two recent *in vivo* ^{31}P NMR studies on *P. brachycephalum* (Mark et al., 2002) and *Gadus morhua* (Sartoris et al., 2003) white muscle confirmed that only moribund animals displayed a drop in pH and $|dG/d\zeta|$ in this tissue at temperatures beyond T_c. Sartoris et al. noted that even immediate cooling could not reverse detrimental changes in tissue energy status (Sartoris et al., 2003).

In our experiments, cuttlefish survived exposure to the high T_c, when rapidly cooled to control temperatures (F.M. and C.B., personal observation), suggesting that the observed net use of the phosphagen reflects an energetic limitation of actively working muscle sections rather than an energetic limitation of all muscle, including the resting bulk of circular and anaerobic ('white') muscle fibres. This emphasizes that active tissues are the first to be affected by temperature-induced oxygen deficiency. Effects in white or passive muscle set in at the end of a progressive oxygen limitation cascade and thus only occur once severe damage to other organs, especially those involved in driving blood circulation, has already set in, leading to ventilatory and circulatory failure as in fish (Van Dijk et al., 1999; Mark et al., 2002). Accordingly, progressive

radial fibre fatigue of the cephalopod mantle characterizes an early limitation in response to temperature. It will eventually affect all other tissues, as oxygen uptake and distribution will likely be negatively affected by decreasing ventilatory pressures (Fig. 6A,B). However, whether radial muscle fatigue observed in our study results from limited ventilatory muscle power output *per se* or is caused by a progressively limited oxygen supply through the blood circulation or by a combination of both processes remains to be established.

This study was carried out in support of the project 'The cellular basis of standard and active metabolic rate in the free-swimming cephalopod, *Sepia officinalis*' (NERC Grant PFZA/004). The authors wish to thank Rolf Wittig and Timo Hirse for their excellent technical support, Raymond and Marie-Paule Chichery (Université de Caen) for providing cuttlefish eggs in 2002 and 2003 and all student helpers that were engaged in raising the animals in our laboratory.

References

Aitken, J. P., O'Dor, R. K. and Jackson, G. D. (2005). The secret life of the giant cuttlefish *Sepia apama* (Cephalopoda): behaviour and energetics in nature revealed through radio acoustic positioning and telemetry (RAPT). *J. Exp. Mar. Biol. Ecol.* **320**, 77-91.

Allen, D. G. and Westerblad, H. (2001). Role of phosphate and calcium stores in muscle fatigue. *J. Physiol*. **536**, 657-665.

Bailey, D. M., Peck, L. S., Bock, C. and Pörtner, H. O. (2003). High-energy phosphate metabolism during exercise and recovery in temperate and antarctic scallops: an in vivo ^{31}P-NMR study. *Physiol. Biochem. Zool.* **76**, 622-633.

Bartol, I. K. (2001). Role of aerobic and anaerobic circular mantle muscle fibers in swimming squid: Electromyography. *Biol. Bull.* **200**, 59-66.

Bock, C., Sartoris, F., Wittig, R.-M. and Pörtner, H. O. (2001). Temperature-dependent pH regulation in stenothermal antarctic and eurythermal temperate eelpout (Zoarcidae): an *in vivo* NMR study. *Polar Biol.* **24**, 869-874.

Bock, C., Sartoris, F. J. and Pörtner, H. O. (2002). In vivo MR spectroscopy and MR imaging on non-anaesthetized marine fish: techniques and first results. *Magn. Reson. Imaging* **20**, 165-172.

Bone, Q., Pulsford, A. and Chubb, A. D. (1981). Squid mantle muscle. *J. Mar. Biol. Assoc. UK* **61**, 327-342.

Bone, Q., Brown, E. R. and Travers, G. (1994a). On the respiratory flow in the cuttlefish *Sepia officinalis*. *J. Exp. Biol.* **194**, 153-165.

Bone, Q., Brown, E. R. and Usher, M. (1994b). The structure and physiology of cephalopod muscle fibres. In *Cepahlopod Neurobiology* (ed. N. J. Abbot, R. Williamson and L. Maddock), pp. 301-329. Oxford: Oxford University Press.

Borger, R., De Boeck, G., Van Auderke, J., Domisse, R., Blust, R. and Van den Linden, A. (1998). Recovery of the energy metabolism after a hypoxic challenge at different temperature conditions: a ^{31}P nuclear magnetic resonance spectroscopy study with common carp. *Comp. Biochem. Physiol.* **120A**, 143-150.

Boucaud-Camou, E. and Boismery, J. (1991). The migrations of the cuttlefish (*Sepia officinalis* L.) in the English Channel. In *Acta of the 1st International Symposium on the Cuttlefish Sepia* (ed. E. Boucaud-Camou), pp. 179-189. Caen: Université de Caen Publications.

Buck, L. T., Hochachka, P. W., Schon, A. and Gnaiger, E. (1993). Microcalorimetric measurement of reversible metabolic suppression induced by anoxia in isolated hepatocytes. *Am. J. Physiol.* **265**, R1014-R1019.

Burton, R. F. (2002). Temperature and acid–base balance in ectothermic vertebrates: the imidazole alphastat hypothesis and beyond. *J. Exp. Biol.* **205**, 3587-3600.

Chih, C. P. and Ellington, W. R. (1985). Metabolic correlates of intracellular pH change during rapid contractile activity in a molluscan muscle. *J. Exp. Zool.* **236**, 27-34.

Cocking, A. W. (1959). The effects of high temperature on roach (*Rutilus rutilus*). 1. The effects of temperature increasing at a known constant rate. *J. Exp. Biol.* **36**, 217-226.

Combs, C. A. and Ellington, W. R. (1995). Graded intracellular acidosis produces extensive and reversible reductions in the effetive free energy changes of ATP hydrolysis in a molluscan muscle. *J. Comp. Physiol. B* **165**, 203-212.

Combs, C. A. and Ellington, W. R. (1997). Intracellular sodium homeostasis in reaction to the effective free-energy change of ATP hydrolysis: studies of crayfish muscle fibers. *J. Comp. Physiol. B* **167**, 563-569.

Debold, E. P., Dave, H. and Fitts, R. H. (2004). Fiber type and temperature dependence of inorganic phosphate: imlications for fatigue. *Am. J. Physiol.* **287**, C673-C681.

Doumen, C. and Ellington, W. R. (1992). Intracellular free magnesium in the muscle of an osmoconforming marine invertebrate: measurement and effect of metabolic and acid–base pertubations. *J. Exp. Zool.* **261**, 394-405.

Finke, E., Pörtner, H. O., Lee, P. G. and Webber, D. M. (1996). Squid (*Lolliguncula brevis*) life in shallow waters: oxygen limitation of metabolism and swimming performance. *J. Exp. Biol.* **199**, 911-921.

Fitts, E. (1994). Cellular mechanisms of muscle fatigue. *Physiol. Rev.* **74**, 49-94.

Frederich, M. and Pörtner, H. O. (2000). Oxygen limitation of thermal tolerance defined by cardiac and ventilatory performance in spider crab, *Maja squinado*. *Am. J. Physiol.* **279**, R1531-R1538.

Gaede, G. (1980). Biological role of octopine formation in marine molluscs. *Mar. Biol. Lett.* **1**, 121-135.

Hardewig, I., Van Dijk, P. L. M. and Pörtner, H. O. (1998). High energy turnover at low temperatures: recovery from exhaustive exercise in Antarctic and temperate eelpouts. *Am. J. Physiol.* **274**, R1789-R1796.

Heath, A, G. and Hughes, G. M. (1973). Cardiovascular and respiratory changes during heat stress in the rainbow trout (*Salmo gairdneri*). *J. Exp. Biol.* **59**, 323-338.

Hibberd, M. G., Dantzig, J. A., Trentham, D. R. and Goldman, Y. E. (1985). Phosphate release and force generation in skeletal muscle fibres. *Science* **228**, 1317-1319.

Hochachka, P. W. (2000). Pinniped diving response mechanisms and evolution: A window on the paradigm of comparative biochemistry and physiology. *Comp. Physiol. Biochem.* **126A**, 435-458.

Hochachka, P. W. and Somero, G. N. (2002). *Biochemical Adaptation.* Oxford: Oxford University Press.

Hubley, M. J., Locke, B. R. and Moerland, T. S. (1997). Reaction-diffusion analysis of the effects of temperature on high-energy phosphate dynamics in goldfish skeletal muscle. *J. Exp. Biol.* **200**, 975-988.

Jansen, M. A., Shen, H., Zhang, L., Wolkowicz, P. E. and Balschi, J. A. (2003). Energy requirements for the Na^+ gradient in the oxygenated isolated heart: effect of changing the free energy of ATP hydrolysis. *Am. J. Physiol.* **285**, H2437-H2445.

Kammermeier, H. (1987). High energy phosphate of the myocardium: concentration versus free energy change. *Basic Res. Cardiol.* **82**, S31-S36.

Kammermeier, H. (1993). Efficiency of energy conversion from metabolic substrates to ATP and mechanical and chemiosmotic energy. *Basic Res. Cardiol.* **88**, 15-20.

Kammermeier, H., Schmidt, P. and Jüngling, E. (1982). Free energy change of ATP-hydrolysis: a causal factor of early hypoxic failure of the myocardium? *J. Mol. Cell. Cardiol.* **14**, 267-277.

Kost, G. J. (1990). PH standardization for phosphorus – 31 magnetic resonance heart spectroscopy at different temperatures. *Magn. Res. Med.* **14**, 496-506.

Lannig, G., Bock, C., Sartoris, F. J. and Pörtner, H. O. (2004). Oxygen limitation of thermal tolerance in cod, *Gadus morhua* L. studied by magnetic resonance imaging (MRI) and on-line venous oxygen monitoring. *Am. J. Physiol.* **287**, R902-R910.

Mark, F. C., Bock, C. and Pörtner, H. O. (2002). Oxygen – limited thermal tolerance in Antarctic fish investigated by MRI and ^{31}P – MRS. *Am. J. Physiol.* **283**, R1254-R1262.

Messenger, J. B., Nixon, M. and Ryan, K. P. (1985). Magnesium chloride as an anaesthetic for cephalopods. *Comp. Biochem. Physiol.* **82C**, 203-205.

Mommsen, T. P., Ballantyne, J., Macdonald, D, Gosline, J. and Hochachka, P. W. (1981). Analogues of red and white muscle in squid mantle. *Proc. Natl. Acad. Sci. USA* **78**, 3274-3278.

Milligan, B. J., Curtin, N. A. and Bone, Q. (1997). Contractile properties of obliquely striated muscle from the mantle of squid (*Alloteuthis subulata*) and cuttlefish (*Sepia officinalis*). *J. Exp. Biol.* **200**, 2425-2436.

Peck, L. S., Pörtner, H. O., Hardewig, I. (2002). Metabolic demand, oxygen supply and critical temperatures in the Antarctic bivalve, *Laternula elliptica*. *Physiol. Biochem. Zool*. **75**, 123-133.

Pörtner, H. O. (1987). Contributions of anaerobic metabolism to pH regulation in animal tissues: theory. *J. Exp. Biol.* **131**, 69-87.

Pörtner, H. O. (1990). Determination of intracellular buffer values after metabolic inhibition by fluoride and nitrilotriacetic acid. *Respir. Physiol.* **81**, 275-288.

Pörtner, H. O. (1994). Coordination of metabolism, acid-base regulation, and haemocyanin function in cephalopods. *Physiology of Cephalopod Molluscs – Lifestyle and Performance Adaptations* (ed. H. O. Pörtner, R. K. O'Dor and D. MacMillan), pp. 131-148. Basel: Gordon and Breach.

Pörtner, H. O. (2001). Climate change and temperature dependent biogeography: oxygen limitation of thermal tolerance in animals. *Naturwissenschaften* **88**, 137-146.

Pörtner, H. O. (2002a). Climate change and temperature dependent biogeography: systemic to molecular hierarchies of thermal tolerance in animals. *Comp. Biochem. Physiol.* **132A**, 739-761.

Pörtner, H. O. (2002b). Environmental and functional limits to musclular exercise and body size in marine invertebrate athletes. *Comp. Biochem. Physiol.* **133A**, 303-321.

Pörtner, H. O., Boutilier, R. G., Tang, Y. and Toews, D. P. (1990). Determination of intracellular pH and PCO_2 after metabolic inhibition by fluoride and nitrilotriacetic acid. *Respir. Physiol*. **81**, 255-274.

Pörtner, H. O., Webber, D. M., Boutilier, R. G. and O'Dor, R. K. (1991). Acid–base regulation in exercising squid (*Illex illecebrosus*, *Loligo paelei*). *Am. J. Physiol.* **261**, R239-R246.

Pörtner, H. O., Webber, D. M., O'Dor, R. K. and Boutilier, R. G. (1993). Metabolism and energetics in squid (*Illex illecebrosus*, *Loligo pealei*) during muscular fatigue and recovery. *Am. J. Physiol.* **265**, R157-R165.

Pörtner, H. O., Finke, E. and Lee, P. G. (1996). Metabolic and energy correlates of intracellular pH in progressive fatigue of squid (*L. brevis*) mantle muscle. *Am. J. Physiol.* **271**, R1403-R1414.

Pörtner, H. O., Peck, L., Zielinski, S. and Conway, L. Z. (1999). Intracellular pH and energy metabolism in the highly stenothermal antarctic bivalve *Limopsis marionensis* as a function of ambient temperature. *Polar Biol.* **22**, 17-30.

Reeves, R. B. (1972). An imidazole alphastat hypothesis for vertebrate acid–base regulation: tissue carbon dioxide content and body temperature in bullfrogs. *Respir. Physiol.* **14**, 219-236.

Sartoris, F. J., Bock, C., Serendero, I., Lannig, G. and Pörtner, H. O. (2003). Temperature-dependent changes in energy metabolism, intracellular pH and blood oxygen tension in the Atlantic cod. *J. Fish. Biol.* **62**, 1239-1253.

Sokolova, I. M. and Pörtner, H. O. (2003). Metabolic plasticity and critical temperatures for aerobic scope in a eurythermal marine invertebrate (*Littorina saxatilis*, Gastropoda: Littorinidae) from different latitudes. *J. Exp. Biol.* **206**, 195-207.

Sommer, A., Klein, B. and Pörtner, H. O. (1997). Temperature induced anaerobiosis in two populations of the polychaete worm *Arenicola marina* (L.). *J. Comp. Physiol. B* **167**, 25-35.

Storey, K. B. and Storey, J. M. (1979). Octopine metabolism in the cuttlefish, *Sepia officinalis*: octopine production by muscle and ist role as an aerobic substrate for non-muscular tissues. *J. Comp. Physiol.* **131**, 311-319.

Teague, W. E. and Dobson, G. P. (1992). Effect of temperature on the creatine kinase equilibrium. *J. Biol. Chem.* **267**, 14084-14093.

Tompsett, D. H. (1939). *Sepia.* Liverpool: LMBC Memoirs, Liverpool University Press.

Van Dijk, P. L. M., Hardewig, I. and Pörtner, H. O. (1997). Temperature dependent shift of pHi in fish white muscle: contributions of passive and active processes. *Am. J. Physiol.* **272**, R84-R89.

Van Dijk, P. L. M., Tesch, C., Hardewig, I. and Pörtner, H. O. (1999). Physiological disturbances at critically high temperatures: a comparison between stenothermal Antarctic and eurythermal temperate eelpouts (Zoarcidae). *J. Exp. Biol.* **202**, 3611-3621.

Wannenburg, T., Janssen, P. M. L., Fan, D. and De Tombe, P. P. (1997). The Frank Starling mechanism is not mediated by changes in rate of cross-bridge detachment. *Am. J. Physiol.* **273**, H2428-H2435.

Webber, D. M. and O'Dor, R. K. (1986). Monitoring the metabolic rate and activity of free-swimming squid with telemetered jet pressure. *J. Exp. Biol.* **126**, 205-224.

Wells, M. J. and Wells, J. (1982). Ventilatory currents in the mantle of cephalopods. *J. Exp. Biol.* **99**, 315-330.

Wells, M. J. and Wells, J. (1991). Is *Sepia* really an octopus? In *Acta of the 1st International Symposium on the Cuttlefish Sepia* (ed. E. Boucaud-Camou), pp. 77-92. Caen: Université de Caen Publications.

Zielinski, S. (1999). Consequences of high metabolic rates in cephalopods from different geographical latitudes. *Berl. Polarforsch.* **338**, 198.

Zielinski, S. and Pörtner, H. O. (1996). Energy metabolism and ATP free-energy change of the intertidal worm *Sipunculus nudus* below a critical temperature. *J. Comp. Physiol. B* **166**, 492-500.